

# Analysis of simultaneous influence of operating variables on abrasive wear of phenolic composites

Bhabani K. Satapathy, Jayashree Bijwe\*

*Industrial Tribology Machine Dynamics and Maintenance Engineering Centre (ITMMEC), Indian Institute of Technology, New Delhi 110016, India*

Received 5 October 2001; received in revised form 23 April 2002; accepted 27 May 2002

---

## Abstract

The paper deals with the abrasive wear investigations on various composites of phenolic resin filled with alumina powder and abraded against silicon carbide paper under dry and single pass condition. The data analysis was done using orthogonal experimental design method. The objective was to study the influence of variables such as filler concentration, load, sliding speed and abrading particle size on the abrasive wear performance of phenol-formaldehyde-based composites. Regression analysis of the data was carried out to develop equations for the composites in which the wear volumes of the specimens were expressed in terms of simultaneous contribution from the influence of load, abrading particle size, sliding speed and their mutual interactions. It was confirmed that among these factors load was the factor contributing most strongly to the wear of these composites. Sliding speed seemed to have least effect on the wear performance in the selected operating conditions. Worn surfaces were studied by scanning electron microscopy (SEM) and energy dispersive X-ray analysis (EDAX) to have an insight into the wear mechanisms and particle dispersion in the bulk of the composites.

*Keywords:* Phenolics; Abrasive wear; Alumina; Composites

---

## 1. Introduction

Ceramic particulate filled phenolic composites are of special significance because of their applications in friction linings. Ceramic particulate fillers such as alumina, quartz, flint and silica serve as a major class of fillers in the friction materials because of their high-temperature resistance, better integrity with the resin, and beneficial influence on friction and wear of friction materials [1-4]. The major contributing wear mechanisms in the wear of friction materials are adhesive, abrasive, fatigue and impact [5]. The composition of friction materials and its processing is a guarded technology and the literature is commercially sensitive. Numerous types and combinations of abrasives in various percentages have been used in friction material. However, the patent literature reports on the overall performance of a multi-ingredient composite materials rather than highlighting on the influence of individual class of materials. A little is reported on systematic studies on the influence of various abrasives such as alumina, silica and quartz etc. on the friction and wear performance of binary phenolic composites [6]. Moreover, analysis of simultaneous influence of various

operating parameters has not yet been studied in this respect. On the contrary, in the case of anti-friction materials such as UHMWPE, polyamides and PEI composites such efforts have been reported and proved very useful for fundamental and comprehensive understanding of the extent of influence of the various parameters on abrasive wear of composites [7,8]. Analyses were also made to develop an improved understanding of wear behaviour of blends and alloys, such as PA-6/UHMWPE alloys and blends [9]. In this scenario, such efforts are also required for thermosetting composites.

Since alumina is the most widely used abrasive in friction material, such efforts were focussed on alumina-filled phenolic composites. Wear behaviour of these composites in abrasive condition has not been reported so far, though data on their influence on the mechanical properties have been available [10]. Investigations on wear performance and analysis of results are presented in the following sections.

## 2. Experimental details

### 2.1. Materials and preparation

Phenolic resin of novolak type (HR 6152) from Bakelite-Hylam Limited, India with an average particle size of 150 mesh and with 8-10% hexamine content was selected as

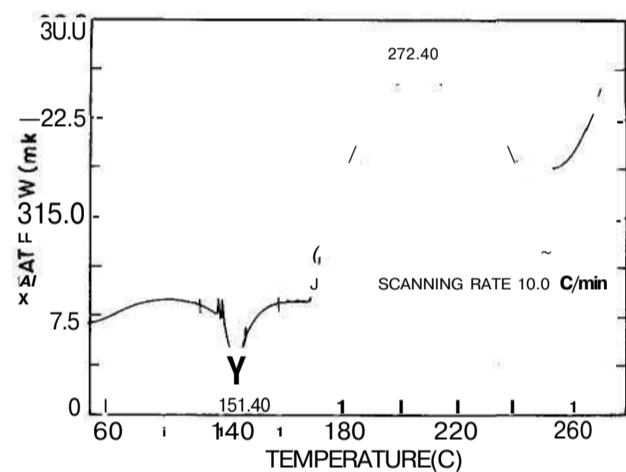


Fig. 1. DSC curve of phenol-formaldehyde resin showing its curing temperature (in air at 10°C/min; Perkin-Elmer Instrument).

base material while alumina of particle size in the range 48-100  $\mu\text{m}$  with a particle density of  $3.96 \text{ g cm}^{-3}$  was selected as a filler. The filler was homogeneously mixed in the phenolic powder in a domestic mixer in various percentages (5, 10, 15 and 20%) in four different batches. The DSC curve as shown in Fig. 1 indicated its curing temperature in the range 150-153 °C. The filler-resin mixtures were then compression moulded at a curing temperature of 153 °C for 15 min under a pressure of 15 MPa with two intermittent breathings to expel the volatiles out. Sample bars of dimensions 120 mm x 60 mm x 6 mm were then post-cured at a temperature of 100 °C in the oven for 10 h. Sample pins of diameter 6 mm were cut from the samples for tribo-studies. The compositions and the physical properties of the samples are listed in Table 1. Hardness was measured on Scleroscope hardness tester while tensile strength was measured on Zwick Z010 machine.

## 2.2. Abrasive wear test

Wear tests were carried out on a single-pin-on-disc machine described elsewhere [11]. A small pin sample of 6 mm diameter and 6 mm height was abraded against silicon carbide (SiC) waterproof abrasive paper of 1200 grade in dry condition for uniform contact. Two grades of SiC abrasive papers, with mean abrasive particle size of 90 and 175  $\mu\text{m}$  corresponding to grades 80 and 120, respectively, were

Table 1  
Details of selected phenolic based materials

Specimen	Al <sub>2</sub> O <sub>3</sub> content (wt.%)	Density ( $\text{g cm}^{-3}$ )	Hardness (scleroscopy)	Tensile strength (MPa), ASTM D 638
1	0	1.300	45	10.76
2	5	1.345	53	12.22
3	10	1.393	48	8.21
4	15	1.445	55	16.70
5	20	1.500	60	14.18

selected as the abrading counterfaces. The experiments were carried out on a circular wear track of radius 50 mm by testing for one revolution on the abrasive disk, thereby achieving a total distance of 3.2 m after changing required number of fresh papers. The selected loads were 6, 8, 10 and 12 N. Two different speeds, 50 and 80  $\text{r min}^{-1}$  were also selected as the operating variables. Each experiment was repeated three times and the mean value of weight loss was taken. Specific wear rate ( $K_0$ ) was calculated from the following equation:

$$K_0 = \frac{\Delta m}{\rho L D} \quad (\text{m}^3 \text{N}^{-1} \text{m}^{-1})$$

where  $\Delta m$  is the weight loss in g,  $\rho$  the density in  $\text{g cm}^{-3}$ ,  $L$  the load in Newton and  $D$  the abrading distance in m. For the analytical treatment of the data, wear was expressed in terms of wear volume and the data generated under three loads, 8, 10 and 12 N were used for designing the experiments for analysis.

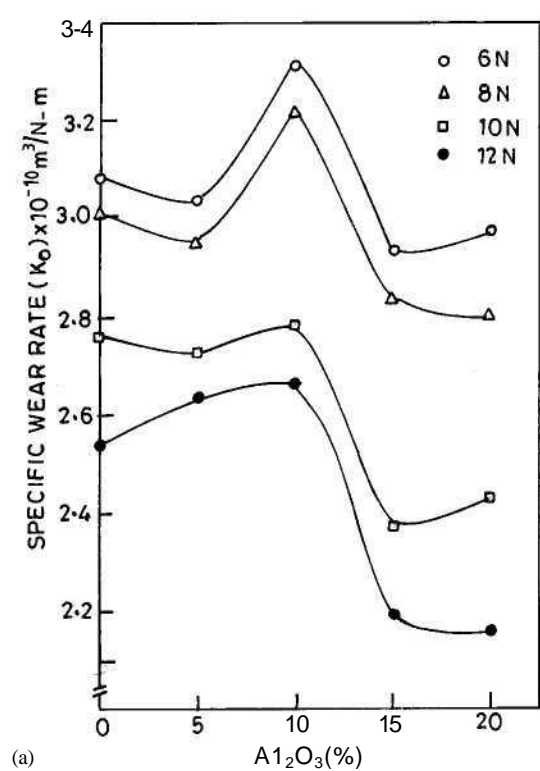
The worn surfaces were gold coated and examined with a JEOL JSM-840 scanning electron microscope (SEM) and Philips 515 SEM attached with energy dispersive X-ray analyser (EDAX).

## 3. Results and discussion

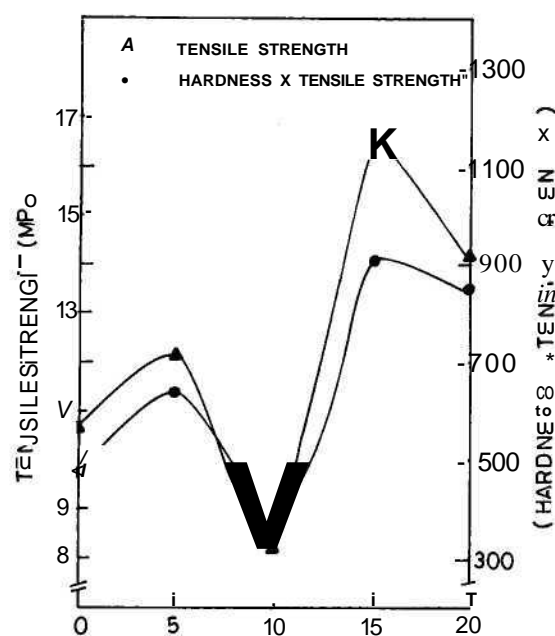
### 3.1. Wear rate and correlation

Specific wear rate of the composites abraded under specified conditions under different loads and 175  $\mu\text{m}$  grit size are expressed as a function of filler percentages in Fig. 2a. The tensile strength ( $S$ ) and the product of hardness and tensile strength ( $HS$ ) are plotted against the filler concentration in Fig. 2b to investigate the possible existence of correlation between mechanical properties and the specific wear rates of the composites. Similar trends were observed in these relations in case of the specific wear rates for abrasion against 90  $\mu\text{m}$  SiC paper, and hence they are not shown in a separate figure. SEM micrographs of worn surfaces of composites are collected in Fig. 3.

The specific wear rates of the selected materials were of the order of  $10^{-10} \text{ m}^3 \text{N}^{-1} \text{m}^{-1}$ . It is evident from Fig. 2a that among all the compositions the 10% filled phenolic composite showed a maximum in specific wear rate ( $K_0$ ) under all the loads. This was consistent with their corresponding  $HS$  and  $S$  values, which were comparatively higher than the other composites. It was observed that the specific wear rates showed an increasing trend up to 10% alumina loading, followed by a sudden decrease at 15% filler loading. After showing minimum wear at 15%, in most cases the wear subsequently increased for further filler loading, i.e. 20%, but with negligible rate. Thus the most interesting information revealed from the studies is the optimum percentage of filler for enhancement in wear performance. Interestingly, a lower percentage of filler up to 10% did not improve the performance over unfilled material. At 15% alumina inclusion,



(a)



(b)

Fig. 2. (a) Specific wear rate as a function of Al<sub>2</sub>O<sub>3</sub> concentration at different loads (grit size of SiC paper: 80; speed: 5 cm/s; distance abraded: 3.2m); (b) tensile strength (*S*) and the product of tensile strength and hardness (*HS*) as a function of % of Al<sub>2</sub>O<sub>3</sub>.

approximately 15% improvement over the wear behaviour of unfilled matrix was observed at all loads. It therefore, appeared that 15% Al<sub>2</sub>O<sub>3</sub> filler loading might be the ideal amount to formulate the wear resistant composite.

Comparison of Fig. 2a and b revealed that a fairly good correlation existed between wear rate and tensile strength (*S*) and the product of tensile strength and hardness (*HS*). Higher the *S* and *HS* factor, lower was the wear rate. The 15% alumina-filled composite showed the lowest wear rate and the highest values of *S* and *HS*. Though both these factors showed similar trends with wear performance, *HS* parameter appeared to be more influential. The extent of changes in wear rate of composites more closely matched with *HS*.

The specific wear rates showed a decrease with the increase in applied load for all the composites. However, the extent of decrease in the specific wear rate with load was not uniform. This may be attributed to the fact that the operating variables interact simultaneously in a complex manner in a true abrasive situation. It was also observed that as the load was increased, the deviation in the specific wear rates tended to stagnate in all the samples.

### 3.2. Worn surface studies of composites

The surfaces of some composites worn under 12 N load are shown as SEM micrographs in Fig. 3. The characteristic features apparent on the worn surfaces are: development of fatigue cracks in the direction transverse to the abrasion, wavy patterns marked by the circles of the fine cracks, absence of plastic deformations as evident from the sides of the furrows and material removal by brittle fracture. Phenolic matrix being thermoset the energy absorption is less as compared to the thermoplastics. This leads to the development of the various types of cracks on the surface, for example, fatigue cracks as is evident from micrographs, Fig. 3a-f, representing 0% (neat resin), 5, 15 and 20% Al<sub>2</sub>O<sub>3</sub> filled composites. Similarly, wide cracks were observed in 15% Al<sub>2</sub>O<sub>3</sub> filled phenolic composite as shown in Fig. 3e. A general topography of the worn surface with 5% Al<sub>2</sub>O<sub>3</sub> filled composite is shown in Fig. 3b. In the case of thermosetting composites, cracks initiate at the filler-matrix interface and propagate very easily through the matrix towards the other filler-matrix interfaces. When the network of cracks intersects, the filler particle becomes loose and are removed in the form of wear debris. The resin also gets removed in the form of fine wear debris caused by brittle fracture of the resin. Thus the material removal is easier for thermosets than for thermoplastics. Fig. 3f shows 20% filler composite. The corresponding EDAX image for Fig. 3f is in Fig. 3g and indicates the distribution pattern of alumina in the form of Al dot density. Higher percentage of filler may lead to less widely distributed particles, which in turn reduces the inter-particle distance.

### 3.3. Analysis of abrasive wear data

In order to understand the complex interacting modes of the operating variables and their individual contributions to

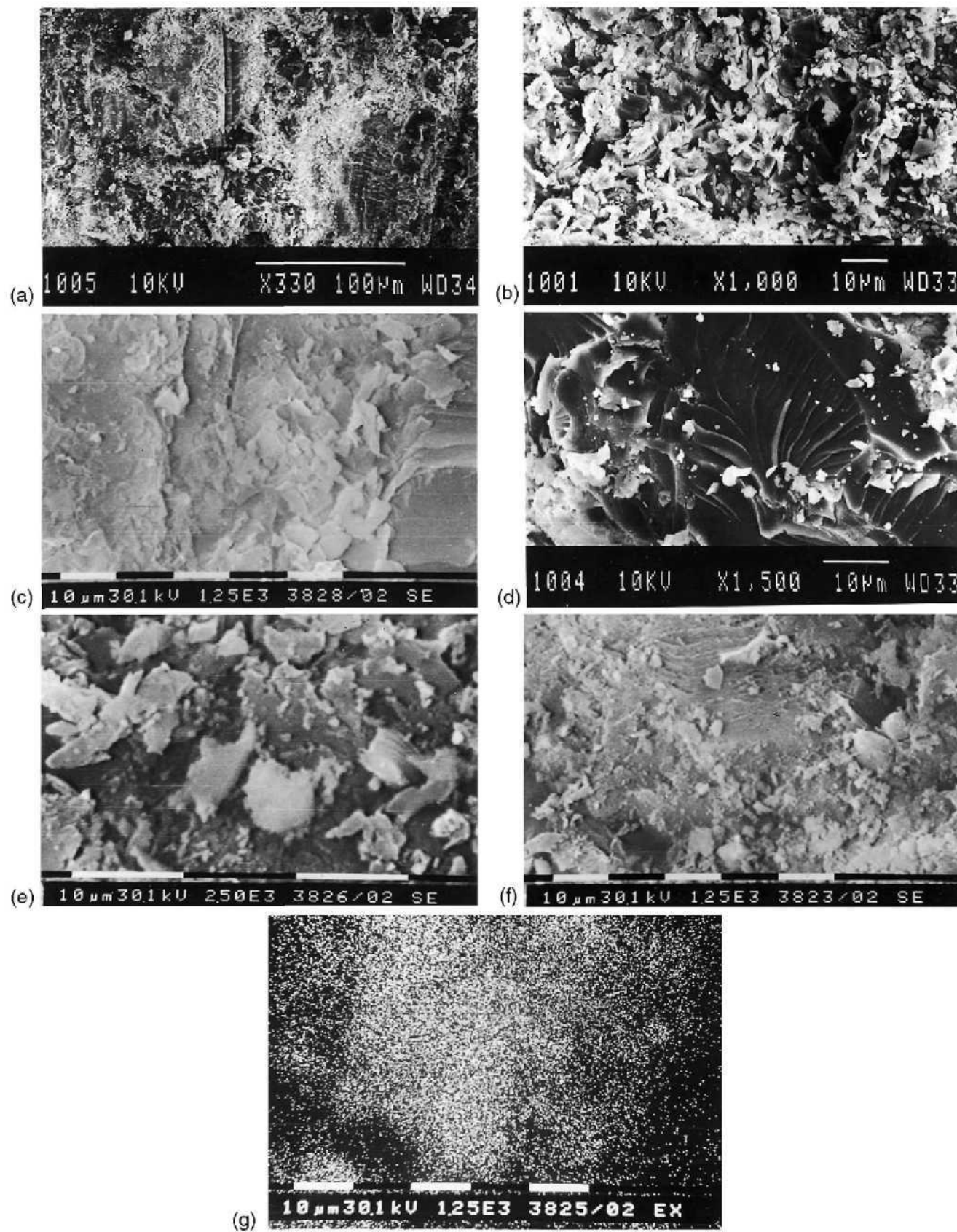


Fig. 3. SEM micrographs of worn surfaces (80 grade SiC paper under 12N load): (a) neat resin; (b) 5% Al<sub>2</sub>O<sub>3</sub> filled composite; (c) 5% Al<sub>2</sub>O<sub>3</sub> filled composite with fatigue marks; (d) 15% Al<sub>2</sub>O<sub>3</sub> filled composite; (e) 15% Al<sub>2</sub>O<sub>3</sub> filled composite showing microcracks; (f) 20% Al<sub>2</sub>O<sub>3</sub> filled composite with fatigue cracks; (g) EDAX micrograph of 20% Al<sub>2</sub>O<sub>3</sub> filled phenolic composite.

Table 2  
The investigated parameters and their test levels

Investigated parameters	Sliding speed Z <sub>1</sub> (ms <sup>-1</sup> )	Abrasive particle size Z <sub>2</sub> (μm)	Load Z <sub>3</sub> (N)
Zero level (Z <sub>0</sub> )	–	–	10
High level (+1)	0.08	175	12
Low level (–1)	0.05	90	8
Point space	0.03	85	2

the abrasive wear performance of the composites, regression analysis was carried out based on an orthogonal test design method. Efforts were made to correlate wear volume with load, abrading particle size, sliding speed and their mutual interactions. From this regression equations between volume loss and its affecting factors were elucidated which were subsequently tested for their validity using statistical F-tests at a particular test level.

### 3.3.1. The test arrangement

The contributions of sliding velocity (Z<sub>1</sub>; ms<sup>-1</sup>), abrasive particle size (Z<sub>2</sub>; μm), load (Z<sub>3</sub>; N) and their interactions to the wear were investigated. The investigated parameters and their test levels are listed in Table 2. The orthogonal array L12 (2<sup>2</sup> × 3) was selected to arrange the test program. The test arrangement and results are listed in Table 3.

### 3.3.2. Regression equation between volume loss and its affecting factors

For the convenience of data processing and to calculate the regression coefficient according to the code, the investigated parameters are encoded as following (Eqs. (1a)–(1e)) to give normalised variables varying within the range of [–1,1] [12,13]:

$$X_{11} = \frac{2(Z_1 - \bar{Z}_1)}{A_1} \sim \frac{2(Z_1 - 0.065)}{0.03} \quad (1a)$$

$$X_{12} = \frac{Z_2 - \bar{Z}_2}{A_2} = \frac{Z_2 - 132.5}{85} \quad (1b)$$

$$X_{13} = \frac{Z_3 - \bar{Z}_3}{\Delta_3} = \frac{Z_3 - 10}{2} \quad (1c)$$

$$X_{22} = 3 \left[ \left\{ \frac{Z_2 - \bar{Z}_2}{\Delta_2} \right\}^2 - \frac{N^2 - 1}{12} \right] \\ = 3 \left[ \left\{ \frac{Z_2 - 132.5}{85} \right\}^2 - \frac{12^2 - 1}{12} \right] \quad (1d)$$

$$X_{23} = 3 \left[ \left\{ \frac{Z_3 - \bar{Z}_3}{A_3} \right\}^2 - \frac{N^2 - 1}{12} \right] \\ = 3 \left[ \left\{ \frac{Z_3 - 10}{2} \right\}^2 - \frac{12^2 - 1}{12} \right] \quad (1e)$$

where  $X_{11}$ ,  $X_{12}$  and  $X_{13}$  stand for the first-order codes of sliding velocity, abrasive particle size and load, respectively;  $X_{22}$  and  $X_{23}$  the second-order codes of abrasive particle size and load, respectively.  $A$  is the level space of investigated parameters;  $N$  the test level number of the parameter.  $\bar{Z}$  is the mean value of investigated parameter. The codings of the parameters are summarised in Table 4 with the statistical calculation and regression coefficients  $b_j$ , where  $B_j$ ,  $D_j$ , and  $b_j$  are expressed as follows (Eqs. (2a)–(2c)):

$$B_j = \sum_{i=1}^{12} (X_{ji} y_i) \quad (2a)$$

$$D_j = \sum_{i=1}^{12} (X_{ji}^2) \quad (2b)$$

$$b_j = \frac{B_j}{D_j} \quad (2c)$$

Table 3  
Experimental arrangement and results

S. no.	Z <sub>1</sub>	Z <sub>2</sub>	Z <sub>3</sub>	y <sub>1</sub>	<i>n</i>	y <sub>3</sub>	y*	y <sub>5</sub>
1	0.05	175	8	0.0069	0.0085	0.0086	0.0074	0.0073
2	0.05	175	10	0.009	0.0090	0.0077	0.007	0.0079
3	0.05	175	12	0.01	0.01	0.011	0.0085	0.0085
4	0.05	90	8	0.0062	0.0055	0.0057	0.0058	0.0060
5	0.05	90	10	0.0068	0.00	0.00	0.0061	0.0062
6	0.05	90	12	0.0074	0.007	0.0073	0.0071	0.0069
7	0.08	175	8	0.0081	0.0079	0.0083	0.0087	0.0084
8	0.08	175	10	0.0093	0.0087	0.0091	0.0093	0.0091
9	0.08	175	12	0.0101	0.0098	0.0098	0.010	0.010
10	0.08	90	8	0.0063	0.0051	0.0053	0.0057	0.0052
11	0.08	90	10	0.0077	0.00	0.0063	0.0063	0.0061
12	0.08	90	12	0.0089	0.0073	0.0071	0.0076	0.0071

**Table 4**  
Statistical analysis

Codes	$\Psi_0$	Xn	X12	X22	X13	X23	X11X12	X11X13	X12X13	X22X13	X12X23	X11X12X13
1	1	110	1	0	11	1	11	1	011	0	1	1
2	1	11	1	0	0	-2	-1	0	0	0	-2	0
3	1	11	1	0	1	1	-1	11	1	0	1	-1
4	1	-1	-1	0	11	1	1	1	1	0	-1	-1
5	1	-1	-1	0	0	020	1	0	0	0	2	0
6	1	-1	01	0	1	1	1	-1	-1	0	11	1
7	1	1	1	0	111	1	1	-1	01	0	1	-1
8	1	1	1	0	0	-2	1	0	0	0	-2	0
9	1	1	1	0	1	1	1	1	1	0	1	1
10	1	1	-1	0	11	1	-1	110	1	0	11	1
11	1	1	-1	0	0	-2	-1	0	0	0	2	0
12	1	1	011	0	1	1	11	1	-1	0	-1	-1
Dj	12	12	12	0	8	16	12	8	8	0	16	8
Bj(y1)	0.0976	0.005	0.011	0	0.0098	-0.0008	0	0.0012	0.0022	0	-0.0004	0.065
Bj(y1)	0.0081	0.00041	0.00092	0	0.0008	-0.00005	0	0.00015	0.000275	0	-0.000025	0.008125
Bj(y2)	0.0915	-0.002	0.0163	0	-0.0163	0.0024	-0.0003	0.0004	-0.001	0	-0.0503	0.0004
Bj(y2)	0.0076	-0.00016	0.00135	0	-0.0013	0.00015	-0.000025	0.00003	-0.000125	0	-0.003144	0.00005
Bj(y3)	0.0930	-0.0016	0.1058	0	-0.0176	0.0033	-0.001	-0.0007	0.0005	0	0.0889	0.0871
Bj(y3)	0.0077	-0.00013	0.0088	0	-0.00146	0.0002	-0.000083	-0.00009	0.0000625	0	0.00561	0.0108
Bj(y4)	0.0903	0.0051	0.0131	0	-0.0131	0.0021	0.0039	0.0009	-0.0007	0	-0.0007	-0.0003
Bj(y4)	0.0075	0.00425	0.0011	0	-0.0011	0.0001	0.000325	0.00011	-0.00009	0	-0.000044	-0.0000375
Bj(y5)	0.0887	0.0031	0.0164	0	-0.0137	0.0008	0.0045	0.0014	0	0	-0.0077	-0.0006
Bj(y5)	0.0074	0.00026	0.0014	0	-0.00114	0.00005	0.000375	0.00018	0	0	-0.00048	-0.000075

Based on the results in Table 4 and neglecting the terms having minor influence on the abrasive wear test results, the regression equation between wear ( $y$ ;  $\text{cm}^3$ ) and each individual parameter as well as their interactions can be obtained.

The regression equations between wear and investigated parameters for 0% (neat phenolic), 5, 10, 15 and 20%  $\text{Al}_2\text{O}_3$  filled phenolic composites were expressed as

$$y_1 = 0.0081 + 0.00092X_{12} + 0.0008X_{13} - 0.00005X_{23} + 0.0081X_{11}X_{12}X_{13} \quad (3)$$

$$y_2 = 0.0076 + 0.00135X_{12} - 0.0013X_{13} + 0.00015X_{23} + 0.00005X_{11}X_{12}X_{13} \quad (4)$$

$$y_3 = 0.0077 + 0.0088X_{12} - 0.0015X_{13} + 0.0002X_{23} + 0.0108X_{11}X_{12}X_{13} \quad (5)$$

$$y_4 = 0.0075 + 0.0011X_{12} - 0.0011X_{13} + 0.0001X_{23} - 0.00004X_{11}X_{12}X_{13} \quad (6)$$

$$y_5 = 0.0074 + 0.0014X_{12} - 0.0014X_{13} + 0.00005X_{23} - 0.000075X_{11}X_{12}X_{13} \quad (7)$$

Ignoring the tertiary interdependence factor, in order to avoid the complexities of the calculations, the above equations were reduced to the following forms.

$$y_1 = 0.0081 + 0.00092X_{12} + 0.0008X_{13} - 0.00005X_{23} \quad (8)$$

$$y_2 = 0.0076 + 0.00135X_{12} - 0.0013X_{13} + 0.00015X_{23} \quad (9)$$

$$y_3 = 0.0077 + 0.0088X_{12} - 0.0015X_{13} + 0.0002X_{23} \quad (10)$$

$$y_4 = 0.0075 + 0.0011X_{12} - 0.0011X_{13} + 0.0001X_{23} \quad (11)$$

$$y_5 = 0.0074 + 0.0014X_{12} - 0.0014X_{13} + 0.00005X_{23} \quad (12)$$

Using Eqs. (1a)-(1e), Eqs. (8)-(12) were converted into following equations.

$$y_1 = -0.255 \times Q^{-2} + 2.16 \times 10^{-5}Z_2 + 11.5 \times 10^{-4}Z_3 - 3.75 \times 10^{-5}Z_3^2 \quad (13)$$

$$y_2 = 2.0841 \times 10^{-2} + 3.17 \times 10^{-5}Z_2 - 6.725 \times 10^{-4}Z_3 + 11.25 \times 10^{-5}Z_3^2 \quad (14)$$

$$y_3 = 0.237 \times 10^{-2} + 2.07 \times 10^{-4}Z_2 - 10.5 \times 10^{-4}Z_3 + 15.0 \times 10^{-5}Z_3^2 \quad (15)$$

$$y_4 = 1.687 \times 10^{-2} + 3.429 \times 10^{-3}Z_2 - 5.65 \times 10^{-4}Z_3 + 7.5 \times 10^{-5}Z_3^2 \quad (16)$$

Table 5  
Repeat test results at zero level

Repeat no.	$y_1$	$y_2$	$y_3$	$y_4$	$y_5$
1	0.0088	0.0081	0.0086	0.0079	0.0079
2	0.0091	0.0093	0.0077	0.007	0.0071
3	0.0093	30.00930	0.0081	0.0078	0.0073
4	0.0090	0.0091	0.0088	0.0073	0.0070
5	0.0086	0.0089	50.00860	0.0071	0.0078

$$y_5 = 1.2385 \times 10^{-2} + 3.29 \times 10^{-5} Z_2 - 13.2 \times 10^{-4} Z_3 + 3.75 \times 10^{-5} Z_f \quad (17)$$

In order to estimate the experimental errors, the above equations were tested using the results obtained from repeated tests at zero level (no. 2 run). The repeat results are listed in Table 5. The results are in good agreement with the results obtained from Eqs. (13)–(17) at a degree of confidence of 99% (the confidence level being set at 0.01).

#### 3.4. Discussion

The influence of filler loading on the trends of wear volumes (Table 3) was similar for both the grit sizes, but less pronounced for lower grit size (90  $\mu\text{m}$ ). From the wear regression Eqs. (13)–(17) and Table 4, it was observed that during the abrasive wear process, the parameters such as load  $Z_3$ , abrasive particle size  $Z_2$  and the second-order interference of load  $Z_2$  have certain effects on the wear behaviour of the samples. Among them, load was confirmed to be the predominant influencing factor, followed by the abrasive particle size. In the wear of filled composites, the role of abrasive particle size and load becomes complicated. It was also seen that the role of load abates and the role of abrasive particle size increases with the increase in the filler concentration. In all the cases, the sliding speed  $Z_1$  has little effect on the wear of the samples. From the regression coefficients, it was observed that in the case of neat phenolics, the abrasive particle size and load both contributed synergistically to the wear, though the effect of load was greater. In the cases of composites up to 10% Al<sub>2</sub>O<sub>3</sub>, the regression coefficient of load was greater than that of the abrasive particle size. However, for the 15% Al<sub>2</sub>O<sub>3</sub> filled composite, the regression coefficient for load (5.65) dropped below that of abrasive particle size (34.29). Thus, beyond 10% filler content, the abrasive particle size became the dominant influencing parameter in the wear of the composites, while the load played a secondary role. With further increase in filler (20%), load again proved to be the major parameter influencing the wear process. It was also observed that in the filled composites up to 10% Al<sub>2</sub>O<sub>3</sub>, the regression coefficients for the second-order influence of load increased, and beyond it decreased steadily. This anomalous behaviour of the influence of operating

variables may be attributed to the fact that the surface hardness, toughness, filler-matrix adhesion and the inter-particle distance must have varied with the increase in filler loading. These variations which are responsible for the overall bulk property alterations are not proportional to the filler loading.

#### 4. Conclusions

Inclusion of alumina increased the abrasive wear resistance and tensile strength of a phenolic matrix. About 15% of filler loading was found to be the optimum percentage for higher wear resistance and tensile strength. A clear-cut correlation between wear performance and tensile strength ( $S$ ) and the product of tensile strength and hardness ( $HS$ ) was also observed. Load, speed and grit size were found to be the influencing parameters other than the material properties. However, the analysis of wear data based on regression analysis confirmed that the load was the most influencing contributing factor to the wear process rather than the speed and grit size. Speed was found to be the least influencing parameter in this respect.

#### Acknowledgements

The authors gratefully acknowledge the funding by Department of Science and Technology, New Delhi to carry out this research work.

#### References

- [1] G. Crosa, I.J.R. Baumvol, Tribology of composites used as friction materials, in: K. Friedrich (Ed.), *Advances in Composite Tribology*, Composite Materials Series 8, Elsevier, Amsterdam, 1993, pp. 583-625 (Chapter 16).
- [2] J. Bijwe, Composites as friction materials: recent developments in non-asbestos reinforced friction materials, *Polym. Compos.* 18 (1997) 378-395.
- [3] A.P. Mouritz, D.H. St. John, The abrasive wear properties of some commercial epoxy resin/ceramic composites, in: *Proceedings of the Material Processing and Performance Conference*, Vol. 2-5, Melbourne, Vic., Australia, Sept. 2-5 1991, pp. 210-214.
- [4] F. Qiao, W. Liu, C.S. Huang, Q.J. Xue, Study of abrasive wear of ceramics-reinforced and rubber modified epoxy resin, *Zairyo Gijyutsu (Mater. Technol.)* 11 (8) (1993) 238-243.
- [5] J. Bros, S.F. Scieszka, The investigation of factors influencing dry friction in brakes, *Wear* 41 (1977) 271-286.
- [6] G. Crosa, N. Enderle, H. Leal, A. Oliveira, F.C. Stedile, I.J.R. Baumvol, Study on effect of abrasives on friction material composites, in: *Proceedings of ICAM 91*, May 27-29, Strasbourg, France, 1991, pp. 87-93.
- [7] C. Liu, L. Ren, R.D. Amell, J. Tong, Abrasive wear behaviour of particle reinforced ultra high molecular weight polyethylene composites, *Wear* 225-229 (1999) 199-204.

- [8] M. Fahim, J. Indumathi, J. Bijwe, Statistical data analysis of abrasive wear performance of polyetherimide and composites, *J. Reinf. Plast. Compos.* 20 (12) (2001) 1013-1023.
- [9] C.Z. Liu, L.Q. Ren, J. Tong, T.J.S.M. Green, R.D. Arnell, Statistical wear analysis of PA-6/UHMWPE alloy, UHMWPE and PA-6, *Wear* 249 (2001) 31-36.
- [10] K.C. Hong, M. Ravasi, N. Keil, B. Vigeant, Y. Ma, Effect of organic acids on the mechanical properties of phenolic resin composites, *J. Appl. Polym. Sci.* 76 (5) (2000) 642-647.
- [11] J. Bijwe, C.M. Logani, U.S. Tewari, Influence of fillers and fibre reinforcement on abrasive wear of some polymeric composites, *Wear* 138 (1990) 77-92.
- [12] L.Q. Ren, *Practical Experimental Designs*, Chinese Machinery Press, Beijing, 1986.
- [13] I. Guttman, S.S. Wilks, J.S. Hunter, *Introductory Engineering Statistics*, Wiley, Canada, 1971.